Critical currents, pinning, and edge barriers in narrow $YBa_2Cu_3O_{7-\delta}$ thin films

Shuichi Tahara,* Steven M. Anlage, J. Halbritter,[†] Chang-Beom Eom,[‡] D. K. Fork,
T. H. Geballe, and M. R. Beasley

Department of Applied Physics, Stanford University, Stanford, California 94305

(Received 23 October 1989)

Current transport behavior is reported for narrow strips (down to approximately 1 μm) of $YBa_2Cu_3O_{7-\delta}$ thin films deposited and lithographically patterned by various means. A systematic increase in the critical current densities is observed in the narrowest strips, suggesting the possible presence of an edge barrier-to-flux entry in these films. The critical currents are found to be near the depairing limit as calculated for these particular films. The critical currents are observed to decrease with increasing temperature, consistent with a flux-creep model. Also, current-voltage characteristics are measured at various temperatures. These characteristics are consistent with exponential behavior in the low-temperature region, but are better fit by power-law behavior at the high temperatures. Flux-pinning energies at zero temperature derived from these data range from 20 to 200 meV depending on the method used. The high-temperature power-law behavior may reflect inhomogeneities along the length of the strips.

I. INTRODUCTION

Current transport in thin films of the high-T_c oxide superconductors is of both fundamental and technological interest. It is of particular importance to establish the mechanisms governing the magnitude of the critical current density J_c. Toward this end, it is instructive to measure the current-voltage (I-V) characteristics over a broad range of temperatures, as well as to estimate the critical current density. Especially, transport in narrow strips is informative because it is sensitive to macroscopic inhomogeneities along the films and to the affect of film edges on transport. We have studied the current transport behavior of patterned strips of *in situ* deposited $YBa_2Cu_3O_{7-\delta}$ (Y-Ba-Cu-O) thin films as a function of the strip width in the range of 1–13 μm. We find that high critical current densities J_c can be retained in such narrow strips, and that there is even a systematic increase in J_c in the narrowest strips. At low temperatures the I-V characteristics can be fit either by exponential behavior or power-law behavior. Above ~50 K, the fit to a power law is better. All in all, however, we find the low-temperature behavior is best understood in terms of flux creep, and we use this data to estimate the pinning energies present in these films.

II. SAMPLE PREPARATION, EXPERIMENTAL RESULTS, AND DISCUSSIONS

Thin films of Y-Ba-Cu-O were deposited *in situ* by two means: pulsed laser ablation[1] and single target magnetron sputtering.[2] The substrates used were MgO(100), yttria-stabilized zirconia (YSZ) (100) or $SrTiO_3$ (100). The oxygen pressure and substrate temperature during deposition are 200 mtorr and approximately 700 °C in laser ablation, and 10 mtorr with 40 mtorr Ar mixture and approximately 650 °C in sputter deposition, respec-

tively. Film thicknesses range from 300 to 2200 Å. The I-V characteristics were measured at various temperatures on strips, typically 1–13 μm wide and 1.5 mm long, that had been patterned by standard photoresist lithography and chemical etching using dilute nitric acid or ion milling. Conventional four terminal measurements were used. Critical current densities were determined on the basis of a threshold criterion, the critical voltage being 0.4 μV (~3 μV/cm). The samples studied, their mode of preparation and some of their physical properties are listed in Table I.

For the most part, the critical temperature T_c was not affected by patterning and reflects the intrinsic behavior of the film. For example, as shown in Fig. 1, for most of our laser ablated films the patterned strips exhibit sharp resistive transitions with a constant critical temperature T_c, $\rho(100 \text{ K}) \approx 95$ $\mu\Omega$ cm and $d\rho/dT \approx 0.6$ $\mu\Omega$ cm/K independent of strip width. Such behavior is typical of samples $A1$ to $A3$ and $B1$ to $B3$. In the case of the 300 Å
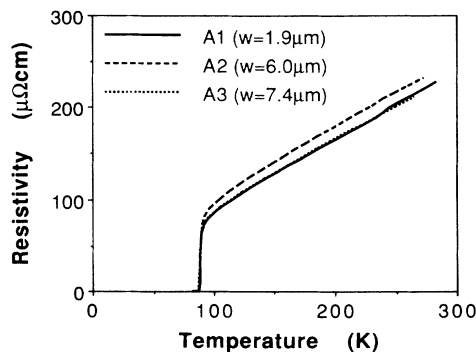
FIG. 1. Resistive transition of laser ablated films of $YBa_2Cu_3O_{7-\delta}$ on YSZ ($d \approx 800$ Å, Sample No. $A1$ to $A3$). The resistive T_c of these samples are approximately 87 K.

TABLE I. List of sample $YBa_2Cu_3O_{7-\delta}$ thin-film preparation conditions and their physical properties. $P(O_2)$ is the pressure of oxygen gas in the chamber, $T(\text{sub})$ is the substrate temperature. Also listed are the film thickness, patterning method, patterned strip width, resistive $T_c(R=0)$, extrapolated critical current density and resistivity at 100 K.

Sample no.	Deposition method	Substrate	$P(O_2)$ (m torr)	T(sub.) (°C)	Thickness (Å)	Patterning method	Width (μm)	T_c (K)	$J_c(0)^a$ (A/cm²)	ρ(100 K) (μΩ cm)
A1	Laser	ZrO_2	200	700	800	CE[b]	1.9	87.5	1.9×10^7	90
A2	Laser	ZrO_2	200	700	800	CE	6.0	87	7.8×10^6	95
A3	Laser	ZrO_2	200	700	800	CE	7.4	86.5	8.2×10^6	90
B1	Laser	$SrTiO_3$	200	700	1200	CE	1.4	86	3.2×10^7	90
B2	Laser	$SrTiO_3$	200	700	1200	CE	4.3	85.5	2.8×10^7	95
C1	Sputter	MgO	10	650	300	CE	5.1	56	1.2×10^6	145
C2	Sputter	MgO	10	650	300	CE	7.1	54	5.0×10^5	130
C3	Sputter	MgO	10	650	300	CE	13.4	56	5.3×10^5	115
D1	Sputter	MgO	10	650	2200	IM[c]	0.85	73.5	2.4×10^7	
D2	Sputter	MgO	10	650	2200	IM	1.9	79	1.6×10^7	95
D3	Sputter	MgO	10	650	2200	IM	4.2	80	1.6×10^7	

[a]Extrapolated critical current densities.
[b]Chemical etching.
[c]Ion milling.

thick films (C1 to C3), T_c decreased approximately by 25 K after etching, and the resistivity showed a dependence on the width. The origin of this deterioration is not clear.

Figure 2 shows the critical current densities of laser ablated films A1 to A3 on YSZ as a function of temperature and strip width. The critical current densities at 10 K of the 1.9-, 6.0-, and 7.4-μm-wide strips are approximately 1.6×10^7, 7.0×10^6, and 8.0×10^6 A/cm², respectively. The critical current density of the narrowest strip is higher than those of the other strips by a factor of 2. This increase in critical current for the narrower strips is also observed in some of the other samples, independent of how they were deposited or patterned, as shown in Table I.

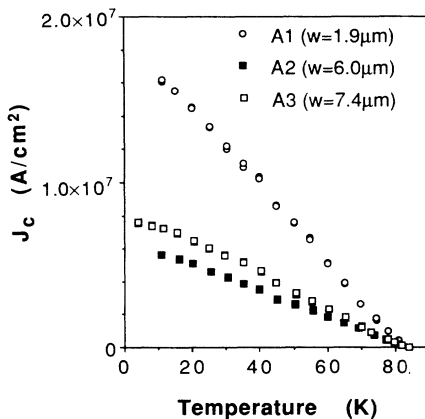The observed independence of the temperature depen-

dence of the resistivity on strip width indicates that no major damage was incurred during lithographic processing, and that few macroscopic inhomogeneities are present in the films. For the wide strips where J_c is independent of strip width, bulk pinning presumably pertains. We believe the increase for the smallest width represents the effect of the edge barrier to vortex entry that is expected to play a role in strips whose width w approaches the transverse penetration depth $\lambda_\perp = \lambda^2/d$, where d is the film thickness. The increase of J_c with decreasing strip width occurs unambiguously in sample series A and C. It is less evident, or even absent, for the others. Note, however, that the thicknesses of samples A and C are less than those of samples B and D. Thus they have significantly larger $\lambda_\perp$'s and would be expected to exhibit larger edge barrier.

The temperature dependence of J_c observed in the strips is very similar to that reported within single Y-Ba-Cu-O grains by Mannhart *et al.*[3] This suggests that the grain boundaries are not determining the critical currents in these films. Like Mannhart *et al.*, we can estimate the pinning energy in the strips by using a flux-creep model. Fits of our data to the flux-creep expression of Tinkham,[4]

$$J_c(t) = J_c(0)(1 - \alpha t - \beta t^2) \tag{1}$$

for small t ($\equiv T/T_c$) yield values of $\alpha \approx 1$ and $\beta \approx 0.3$. The values of the pinning energy $U(0)$ at $T=0$ determined from the expression,

$$\alpha = [kT/U(0)]\ln(E_0/E) ,$$

are also similar to those of Ref. 3 and of order 100 to 200 meV for the better samples as shown in Fig. 3. Here E is the electric-field criterion used to define J_c, E_0 is a characteristic electric field derived in Ref. 3, and k is the Boltzmann constant. We will return later to the question
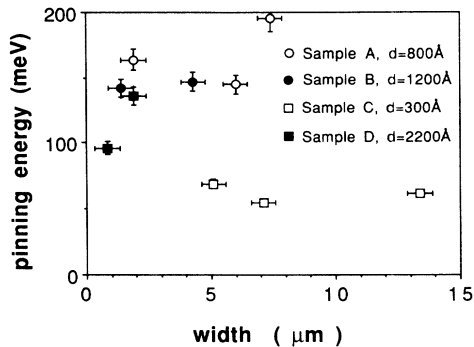

FIG. 2. Temperature dependence of the critical current densities for the laser ablated films of $YBa_2Cu_3O_{7-\delta}$ on YSZ in Fig. 1.

FIG. 3. Pinning energy of the strips vs the strip width for YBa$_2$Cu$_3$O$_{7-\delta}$ thin film. The pinning energies are obtained from the temperature dependence of J_c using the flux-creep formula of Tinkham (Ref. 4).

FIG. 4. Dependence of the critical current density on strip width in YBa$_2$Cu$_3$O$_{7-\delta}$ films. A solid line is a fitting result assuming the critical-state model as a first-order approximation.

of edge barriers versus bulk pinning, but clearly bulk pinning governs J_c in the wider strips. The values below 100 meV correspond to the samples whose T_c's were reduced in the patterning process. We observe a distribution of the pinning energy for a given film (i.e., for different widths) and from film to film.

It is instructive to compare the magnitude of the observed critical current densities with the depairing value J_c^{dp}, and that expected in very narrow strips ($w < \lambda_\perp$) due to the edge barrier J_c^{eb}. It can be shown that in magnitude[5]

$$J_c^{\mathrm{dp}} \approx J_c^{\mathrm{eb}} = c\Phi_0/16\pi^2\lambda^2\xi .\tag{2}$$

Using $\lambda \approx 2500$ Å as measured by our group in similar films[6] and taking $\xi \approx 20$ Å, we obtain $J_c^{\mathrm{eb}} = 1$ to 2×10^8 A/cm^2. In a film thickness of 800 Å, we also obtain $\lambda_\perp \approx 0.75$ μm, which suggests we are not yet in the $w \ll \lambda_\perp$ limit. Nonetheless, it is evident that these films have J_c's approaching their maximum possible values. Moreover, the increase in J_c as w decreases seems clearly related to an edge barrier effect.

Let us estimate the strip width dependence of J_c to first-order assuming the critical state model. According to this assumption, the current density is enhanced at the edges of the film over the value in the center, which is governed by bulk pinning alone. Correspondingly

$$J_c = J_c^e(2a\lambda_\perp/w) + J_c^b ,\tag{3}$$

where J_c^e and J_c^b are the critical current densities corresponding to the edge barrier and to bulk pinning, respectively, and a is an adjustable dimensionless parameter. We assume that these pinning effects are additive. Of course, in the case of $w \ll \lambda_\perp$, the critical current density is expressed as

$$J_c = J_c^e + J_c^b .\tag{4}$$

Figure 4 shows a fit of the data for sample $A1$ to $A3$ to Eq. (3). The fitting parameters are $J_c^b \approx 4.1\times10^6$ A/cm^2
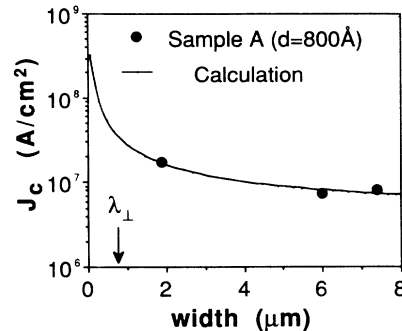
and $J_c^e a\lambda_\perp \approx 1.2\times10^3$ A/cm. If we assume J_c^e is given by Eq. (2), then $a \approx 0.16$.

In Fig. 5, the typical I-V curves are shown for the laser ablated 800-Å thick film $A2$ at seven different temperatures. There exist several schools of thought for the transition from the zero resistance to finite voltage state of the high-temperature superconductors. According to the flux-creep model,[4,7,8] the voltage induced by thermal activation of flux over the pinning barriers is expressed in the low-temperature region as

$$V = V_0\exp[-U(T)/kT + U(0)I/kTI_c(0)] ,\tag{5}$$

where V_0 is a parameter, and $U(0)$ and $I_c(0)$ the extrapolated value of the pinning energy and critical current at $T = 0$. Other points of view include models based on inhomogeneities[9] and a vortex glass[10,11] concept. For both of these models, the V versus I characteristics exhibit a power-law dependence $V \propto I^{\alpha(T)}$. Figures 6(a)–6(d) show the data of Fig. 5 plotted both as $\ln V$-I and $\ln V$-$\ln I$ reflecting these two basic V versus I dependencies. These data are further parametrized in Figs. 7 and 8 where we show the dependence of $d(\ln V)/dI$ versus $1/T$, and $d(\ln V)/d(\ln I)$ versus T. We return to the possible interpretation of these curves in the following.
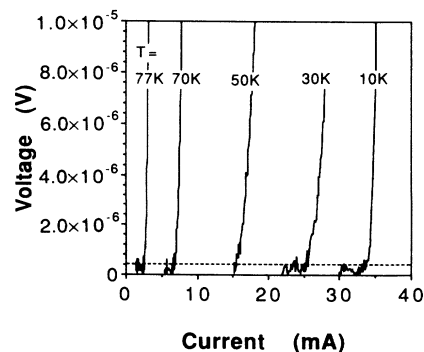

FIG. 5. Current-voltage characteristics of sample $A2$ for various temperatures. Dashed line shows the value of the voltage criterion used for definition of J_c ($V_{\mathrm{crit}} \approx 0.4$ μV).
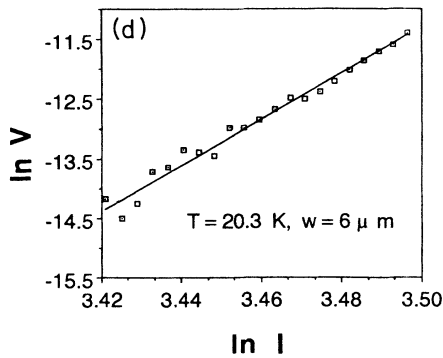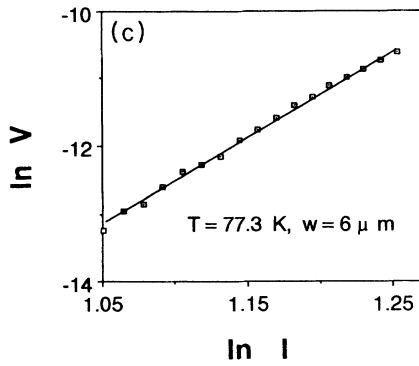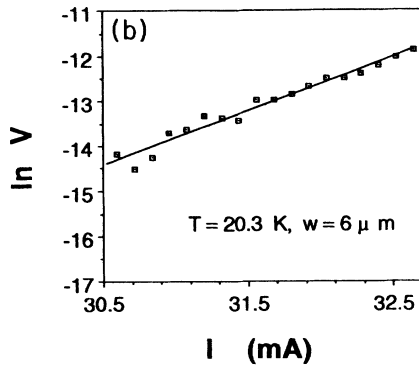
FIG. 7. Experimental relation between $d(\ln V)/dI$ and $1/T$ for samples $A1$ and $A2$. The values of $d(\ln V)/dI$ are obtained from the slope of semilog plots such as Figs. 6(a) and 6(b).

As can be seen in Fig. 6, at low temperatures the data are equally well fit by either an exponential or power-law V versus I relation. At high temperatures, the fit to a power-law dependence is distinctly superior. The cross-over comes about 50–60 K where the temperature dependence of $d(\ln V)/dI$ and $d(\ln V)/d(\ln V)I$ clearly change character. Whether the crossover at this temperature represents an intrinsic temperature behavior or the presence of oxygen deficient regions ($60 \text{ K} < T_c < 90 \text{ K}$) in the films is not entirely clear. In one of our films ($B1$ and $B2$), this change in behavior could be seen directly in the temperature dependence of J_c itself, which would seem to suggest some kind of inhomogeneity.

It is interesting to compare the pinning energy derived from the above-mentioned J_c-T relation with those derived from the I-V characteristics assuming the flux-creep picture. In general, the pinning energy in Eq. (5) depends on the magnetic flux density B. In this experiment, how-
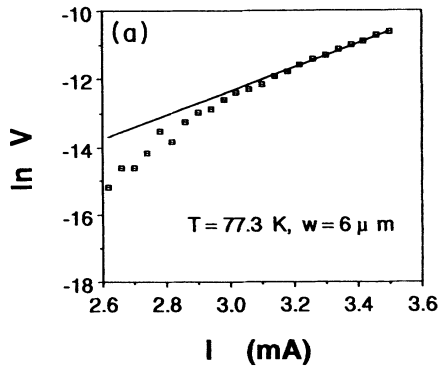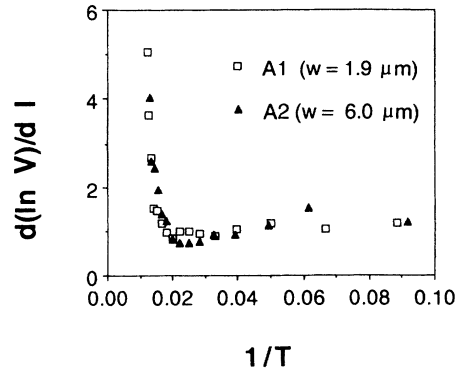

FIG. 6. Typical results for semilog plot and log-log plot in the transition region of the I-V characteristics of sample $A2$. (a) and (c) show those in the high-temperature region, and (b) and (d) are those in the low-temperature region.
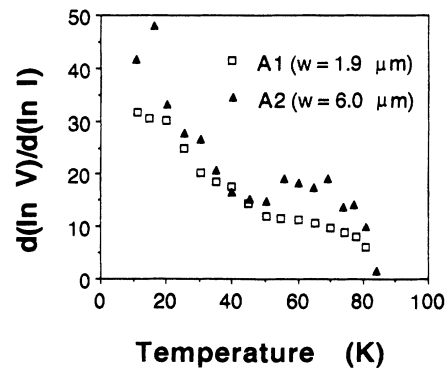

FIG. 8. Experimental data $d(\ln V)/d(\ln I)$ vs temperature. The data show a power-law behavior in the samples $A1$ and $A2$. The values of $d(\ln V)/d(\ln I)$ are found from the slope of log-log plot shown in Figs. 6(c) and 6(d) as examples.

ever, we can neglect the dependence of U on B, as well as that of J_c on B because there is no external magnetic field, and the self-field due to the bias current is of order 10 G at most. Then, at low temperatures the slope of the ln V-I relation is given by

$$d(\ln V)/dI = U(0)/kTI_c(0) \ . \tag{6}$$

In Fig. 7, the experimental relation between $d(\ln V)/dI$ and $1/T$ is shown. As seen in the figures, at low temperatures the values of $d(\ln V)/dI$ increase almost linearly with $1/T$, in agreement with Eq. (6). This agreement, along with the linear temperature dependence of J_c at low temperatures, strengthens the case for a flux-creep interpretation of our data at low temperatures. At higher temperatures, $d(\ln V)/dI$ is seen to increase with temperature. As we have already suggested, the behavior in this regime may reflect inhomogeneities. On the other hand, within the flux-creep model,

$$d(\ln V)/dI \propto U(T)/J_c(T) \propto X(T) \ ,$$

where $X(T)$ is the characteristic length scale over which the pinning energy varies.[12] The data require that $X(T)$ diverges as $T \to T_c$. This is reasonable since both λ and ξ diverge at $T \to T_c$.

From the data of Fig. 7 below 50 K and using Eq. (6), we obtain the pinning energy $U(0) \approx 20$–50 meV for the laser ablated films of different strip width. These values are a factor of 3–5 smaller than the values obtained from the temperature dependence of J_c on the same samples. The voltage range (and hence the rate of flux creep) over which the pinning energies are determined is different for these two measurements, however. Perhaps this can account, in part, for the difference in the inferred pinning energies, the lower values corresponding to the higher transport current. Whether inhomogeneities could play a role here is not known.

It is also interesting to compare the pinning energies found here with those obtained by Ferrari et al.[13] who inferred the distribution of pinning energies in similar Y-Ba-Cu-O in situ thin films from $1/f$ flux noise data. These authors find a distribution that peaks below 100 meV, in acceptable agreement with the values found here.

In interpreting the physical meaning of these pinning energies, it is important to stress that in the experiments reported here, and in the flux noise experiments of Ref. 13, the magnetic fields involved are so small that the vortices in the material are sufficiently far apart that collective effects are not important. It is the depinning energy of individual vortices that is being measured in these experiments. This is in contrast to experiments done in substantial magnetic fields, where interactions between the vortices are important. This same argument rules out vortex glass behavior[10,11] as the origin of the power-law V versus I behavior seen at high temperatures in our samples, since this model depends on the existence of interaction between vortices as we understand it.

Also, we note that the physical interpretation of the pinning energies quoted here is subject to some ambiguities. First, since both edge and bulk pinning are present, it is not obvious a priori which energy (or combination of

the two) we measure. In the widest films this ambiguity is minimal, and it is likely that we measure the bulk pinning energy. Second, it is not known over what length of the vortex the pinning energy pertains. For such thin films, it seems most likely that the vortex moves as a whole along its entire length in any given thermally activated event. In this case, the pinning energy should be proportional to the film thickness. This point was not checked in these experiments, however.

Finally, as we have pointed out above, at high temperatures the I-V characteristics appear to follow a power-law dependence. Plummer et al.[9] have shown that such behavior can follow from a distribution of critical currents along a superconducting filament or strip. In this model,[9]

$$d(\ln V)/d(\ln I) = \alpha(T) = 0.6(J_c/\sigma)^{5/3} \ ,$$

where J_c is the mean critical current density along the filament and σ is the variance in the distribution. Within this picture, the decrease of $\alpha(T)$ with temperature seen in Fig. 8 reflects the decrease of J_c with T. While it is not possible to conclude with certainty that inhomogeneities govern the I-V curves at high temperatures, this interpretation seems plausible, particularly given the possible evidence for some oxygen-deficient regions in our films. In any event, it is clear that there is a distinct change in the behavior of the pinning at ~ 50 K. Also, given the likelihood of some inhomogeneities in these complicated materials, it would seem necessary to rule out inhomogeneities before turning to more intrinsic mechanisms.

III. CONCLUSION

The transport current behavior has been measured in narrow Y-Ba-Cu-O films. An increase of J_c has been observed with decreasing the strip width, even before the width becomes comparable to $\lambda_\perp$. This result suggests the presence of the edge barrier, which impedes the entry of flux into the sample. If we take the strip width smaller than $\lambda_\perp$, it may be possible to reach the transport depairing critical current density ($\approx 4 \times 10^8$ A/cm^2 if we take $\lambda \approx 1500$ Å). We have obtained pinning energies of 50–200 meV from the temperature dependence of J_c, and of 20 to 50 meV from the I-V characteristics in the low-temperature region. The difference of the values of the pinning energies imply the existence of a distribution of pinning energies. We find that the I-V curves of our sample in the high-temperature region exhibit power-law behavior, which may reflect inhomogeneities along the length of the strips.

*Permanent address: Fundamental Research Labs, NEC Corporation, Tsukuba, Japan 305.

†Also at Kernforschungszentrum Karlsruhe, Postfach 3640, D-7500 Karlsruhe 1, Federal Republic of Germany.

‡Department of Materials Science and Engineering, Stanford University, Stanford, CA 94305.

[1]D. K. Fork, K. Char, F. Bridges, S. Tahara, B. Lairson, J. B. Boyce, G. A. N. Connell, and T. H. Geballe, *Proceedings of the International Conference on Materials and Mechanisms of Superconductivity High-Temperature Superconductors* [Physica C **162–164**, 121 (1989)].

[2]C. B. Eom, J. Z. Sun, K. Yamamoto, A. F. Marshall, K. Luther, S. S. Laderman, and T. H. Geballe, Appl. Phys. Lett. **55**, 595 (1989).

[3]J. Mannhart, P. Chaudahari, D. Dimos, C. C. Tsuei, and T. R. McGuire, Phys. Rev. Lett. **61**, 2476 (1988).

[4]M. Tinkham, *Introduction to Superconductivity* (McGraw-Hill, New York, 1975).

[5]K. K. Likharev, Radiofizika **14**, 919 (1971); T. P. Orlando,

Ph.D thesis, Stanford University, 1981.

[6]S. M. Anlage, H. Sze, H. J. Snortland, S. Tahara, B. Langley, C. B. Eom, M. R. Beasley, and R. Taber, Appl. Phys. Lett. **54**, 2710 (1989).

[7]P. W. Anderson and Y. B. Kim, Rev. Mod. Phys. **36**, 39 (1964).

[8]M. R. Beasley, R. Labush, and W. W. Webb, Phys. Rev. **181**, 682 (1969).

[9]C. J. G. Plummer and J. E. Evetts, IEEE Trans. Mag., **MAG-23**, 1179 (1987).

[10]M. P. A. Fisher, Phys. Rev. Lett. **62**, 1415 (1989).

[11]R. H. Koch, V. Foglietti, W. J. Gallagher, G. Koren, A. Gupta, and M. P. A. Fisher, Phys. Rev. Lett. **63**, 1511 (1989).

[12]Only the length scale of the pinning potential enters because, as argued elsewhere in this paper, it is the pinning of individual vortices that we measure here, not so-called flux bundles.

[13]M. J. Ferrari, M. Johnson, F. C. Wellstood, J. Clarke, D. Mitzi, P. A. Rosenthal, C. B. Eom, T. H. Geballe, A. Kapitulnik, and M. R. Beasley, Phys. Rev. Lett. **64**, 72 (1990).